

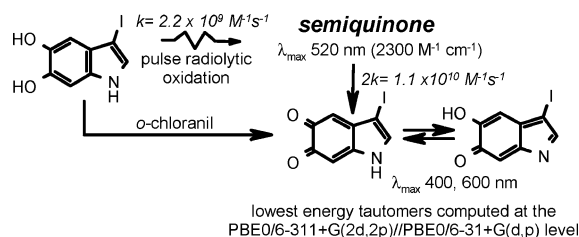
Chemical, Pulse Radiolysis and Density Functional Studies of a New, Labile 5,6-Indolequinone and Its Semiquinone

Alessandro Pezzella,^{*,†} Orlando Crescenzi,^{*,‡} Anna Natangelo,[†] Lucia Panzella,[†]
Alessandra Napolitano,[†] Suppiah Navaratnam,^{§,||} Ruth Edge,^{§,⊥} Edward J. Land,[⊥]
Vincenzo Barone,[‡] and Marco d'Ischia[†]

Department of Organic Chemistry and Biochemistry, University of Naples Federico II, Via Cintia, I-80126 Naples, Italy, Department of Chemistry and INSTM, University of Naples Federico II, Via Cintia, I-80126 Naples, Italy, Free Radical Research Facility, Daresbury Laboratory, Warrington, Cheshire WA4 4AD, United Kingdom, BioSciences Research Institute, University of Salford, Salford M5 4WT, United Kingdom, and Lennard-Jones Laboratories, School of Physical & Geographical Sciences, Keele University, Staffordshire ST5 5BG, United Kingdom

orlando.crescenzi@unina.it; alessandro.pezzella@unina.it

Received July 31, 2006



The chemical and spectroscopic characterization of 5,6-indolequinones and their semiquinones, key transient intermediates in the oxidative conversion of 5,6-dihydroxyindoles to eumelanin biopolymers, is a most challenging task. In the present paper, we report the characterization of a novel, relatively long-lived 5,6-indolequinone along with its semiquinone using an integrated chemical, pulse radiolytic, and computational approach. The quinone was obtained by oxidation of 5,6-dihydroxy-3-iodoindole (**1a**) with *o*-chloranil in cold ethyl acetate or aqueous buffer: it displayed electronic absorption bands around 400 and 600 nm, was reduced to **1a** with Na₂S₂O₄, and reacted with *o*-phenylenediamine to give small amounts of 3-iodo-1*H*-pyrrolo[2,3-*b*]phenazine (**2**). The semiquinone exhibited absorption maxima at 380 nm (sh) and 520 nm and was detected as the initial species produced by pulse radiolytic oxidation of **1a** at pH 7.0. DFT investigations indicated the 6-phenoxy radical and the *N*-protonated radical anion as the most stable tautomers for the neutral and anion forms of the semiquinone, respectively. Calculated absorption spectra in water gave bands at 350 (sh) and 500 nm for the neutral form and at 310 and 360 (sh) nm for the anion. Disproportionation of the semiquinone with fast second-order kinetics ($2k = 1.1 \times 10^{10} \text{ M}^{-1} \text{ s}^{-1}$) gave a chromophore with absorption bands resembling those of chemically generated **1a** quinone. Computational analysis predicted **1a** quinone to exist in vacuo as the quinone–methide tautomer, displaying low energy transitions at 380 and 710 nm, and in water as the *o*-quinone, with calculated absorption bands around 400 and 820 nm. A strong participation of a p orbital on the iodine atom in the 360–380 nm electronic transitions of the *o*-quinone and quinone–methide was highlighted. The satisfactory agreement between computational and experimental electronic absorption data would suggest partitioning of **1a** quinone between the *o*-quinone and quinone–methide tautomers depending on the medium.

Introduction

The 5,6-indolequinones are a highly elusive group of heterocyclic quinones^{1–3} that provide the basic building blocks

of eumelanins, the characteristic brown-to-black insoluble pigments of human skin, hair, eyes, and melanomas.^{4–6} The peculiar ortho dioxygenation pattern present in these quinones

* Corresponding author. Tel: +39-081-674130.

[†] Department of Organic Chemistry and Biochemistry, University of Naples Federico II.

[‡] Department of Chemistry and INSTM, University of Naples Federico II.

[§] Free Radical Research Facility, Daresbury Laboratory.

^{||} BioSciences Research Institute, University of Salford.

[⊥] School of Physical & Geographical Sciences, Keele University.

(1) d'Ischia, M.; Napolitano, A.; Pezzella, A.; Land, E. J.; Ramsden, C. A.; Riley, P. A. *Adv. Heterocycl. Chem.* **2005**, *89*, 1–63.

(2) Il'ichev, Y. V.; Simon, J. D. *J. Phys. Chem.* **2003**, *107*, 7162–7171.

(3) Stark, K. B.; Gallas, J. M.; Zajac, G. W.; Eisner, M.; Golab, J. T. *J. Phys. Chem.* **2003**, *107*, 3061–3067.

(4) Protá, G. *Melanins and Melanogenesis*; Academic Press: San Diego, 1992.

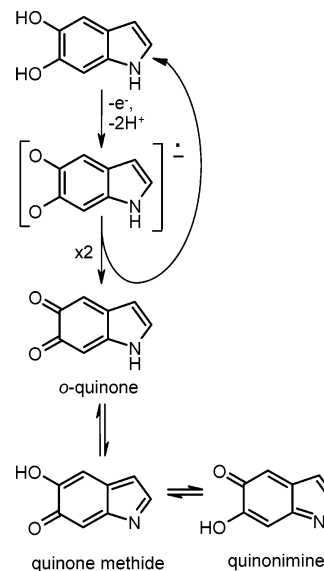
leads to instability in the condensed bicyclic system, resembling that of 2,3-naphthoquinones. This is a consequence of the incompatibility of the dione moiety at the 5,6-positions with the aromatic pyrrole ring, which makes it impossible to write neutral canonical resonance structures with the pyrrole moiety bearing an aromatic sextet.

All attempts at isolating and structurally characterizing the parent 5,6-indolequinone by oxidation of 5,6-dihydroxyindole have so far met with failure, the final outcome being invariably the production of dark, insoluble materials resembling natural eumelanins. In consequence, the chemical and spectroscopic properties of these quinones have long been a matter of speculation and much controversy,⁴ to the point that their existence as independent intermediates in the oxidative polymerization of 5,6-dihydroxyindoles to eumelanin has been questioned.¹

Indirect chemical evidence of the actual existence of 5,6-indolequinone was gained through nucleophilic trapping experiments with sulfhydryl compounds⁷ and thioureyne derivatives.⁸ A first spectral insight into a 5,6-indolequinone was earned by oxidation of 2,3-dimethyl-5,6-dihydroxyindole with *o*-chloranil in CD₃OD⁹ resulting in the development of a species displaying two aromatic singlets at δ 5.47 and 6.26 (1H each) and the signals for the methyl groups at δ 1.47 and 2.02. This compound exhibited a chromophore centered at 360 nm, a lower wavelength than expected from early predictions (see, e.g., the reported identification of the purple pigment “melanochrome”, λ_{\max} 540 nm, with 5,6-indolequinones).¹⁰ On standing, this species gradually decomposed to melanin-like materials, hampering a more complete characterization by spectroscopic techniques. Apart from these efforts, no other direct chemical study of 5,6-indolequinones has appeared so far.

Valuable insights into short-lived intermediates en route to eumelanin polymers have been gained using pulse radiolysis techniques. At pH 7.4, pulse radiolytic oxidation of 5,6-dihydroxyindole leads initially to a transient chromophore with peaks at 330 and 490 nm and a shoulder at 360 nm,¹¹ attributed to a semiquinone radical (Scheme 1). Some uncertainty surrounds the decay of this radical. With pulse radiolysis doses of approximately 20 Gy, decay follows second-order kinetics, consistent with a disproportionation process leading to 5,6-indolequinone and the parent 5,6-dihydroxyindole (Scheme 1). It has been argued¹² that the initial product observed after 5,6-dihydroxyindole semiquinone disproportionation, most likely the *o*-quinone, rapidly isomerizes to the quinone–methide, although a contribution from the quinone–imine was considered.¹¹ Nucleophilic addition of water followed by condensation steps

SCHEME 1. 5,6-Dihydroxyindole Semiquinone Disproportionation Route and Tautomeric Equilibria of the *o*-Quinone



leading to dimers and oligomers have also been considered as possible evolution channels of transient indolequinones under the pulse radiolysis conditions.¹¹

DFT (density functional theory) calculations,² however, predicted the 5,6-indolequinone exists in water almost exclusively as a single *o*-quinone tautomer with no significant absorption in the range 400–600 nm, suggesting that second-order decay of semiquinones may involve other pathways, e.g., dimerization, in addition to disproportionation. There is, however, no definitive chemical evidence that supports either possibility.

As part of ongoing studies toward the synthesis of novel 5,6-dihydroxyindole systems as model building blocks of eumelanin-type polymers,¹ we recently became interested in preparing 5,6-dihydroxy-3-iodoindole (**1a**). The expected electronic and steric effects imparted by the 3-iodo substituent prompted us to investigate this indole as a valuable candidate for a convenient access to a novel 5,6-indolequinone. Besides the academic interest and the relevance to the mechanisms of eumelanin buildup, the chemical and spectroscopic characterization of **1a** quinone was desirable for the prospects of exploring the potential application of this novel indole derivative in materials science, e.g., for the preparation of organic electronics and broadband photon harvesting systems.^{13,14}

We report herein the preparation of **1a**, obtained from the stable *O*-acetyl derivative **1b**, and the first characterization of the corresponding semiquinone and quinone oxidation products by an integrated chemical, pulse radiolysis and DFT approach.

Results and Discussion

Preparation of 1b. 3-Iodoindoles are usually labile and their preparation may be difficult because of the facile loss of iodine during workup.¹⁵ In a previous paper,¹⁶ iodination of 5,6-dihydroxyindole at the 3-position was reported, involving

(5) Protta, G.; d'Ischia, M.; Napolitano, A. In *The Pigmentary System: Its Physiology and Pathophysiology*; Nordlund, J. J., Boissy, R. E., Hearing, V. J., King, R. A., Ortonne, J. P., Eds.; Oxford University Press: New York, 1998; Chapter 24, pp 307–332.

(6) Seagle, B. L.; Rezaei, K. A.; Gasyna, E. M.; Kobori, Y.; Rezaei, K. A.; Norris, J. R., Jr. *J. Am. Chem. Soc.* **2005**, *127*, 11220–11221.

(7) d'Ischia, M.; Napolitano, A.; Protta, G. *Tetrahedron* **1987**, *43*, 5351–5356.

(8) Napolitano, A.; Palumbo, A.; d'Ischia, M.; Protta, G. *J. Med. Chem.* **1996**, *39*, 5192–5201.

(9) Napolitano, A.; Pezzella, A.; d'Ischia, M.; Protta, G. *Tetrahedron Lett.* **1996**, *37*, 4241–4242.

(10) Mason, H. S. *J. Biol. Chem.* **1948**, *172*, 83–92.

(11) Lambert, C.; Chacon, J. N.; Chedekel, M. R.; Land, E. J.; Riley, P. A.; Thompson, A.; Truscott, T. G. *Biochim. Biophys. Acta* **1989**, *993*, 12–20.

(12) Al-Kazwini, A. T.; O'Neill, P.; Adams, G. E.; Cundall, R. B.; Lang, G.; Junino, B. *J. Chem. Soc., Perkin Trans. 2* **1991**, 1941–1945.

(13) Meredith, P.; Powell, B. J.; Riesz, J.; Vogel, R.; Blake, D.; Kartini, I.; Will, G.; Subianto, S. *Broadband photon-harvesting biomolecules for photovoltaics*. In *Artificial Photosynthesis: From Basic Biology to Industrial Application*; Collings, A. F., Critchley, C., Eds.; Wiley-VCH: Weinheim, 2005; Chapter 3, pp 37–65.

(14) Meredith, P.; Powell, B. J.; Riesz, J.; Nighswander-Rempel, S. P.; Pederson, M. R.; Moore, E. G. *Soft Matter* **2006**, *2*, 37–44.

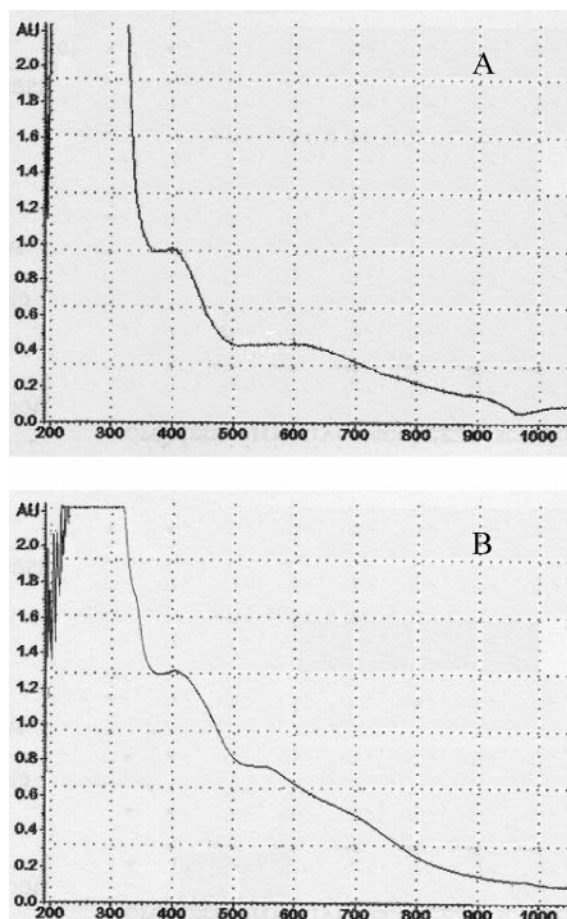


FIGURE 1. Absorption spectra of the oxidation mixture of **1a** by *o*-chloranil in ethyl acetate (trace A) or phosphate buffer pH 7.0 (trace B) at 15 s reaction time. Shown are “baseline subtraction” spectra of the oxidation mixtures. Original spectra are shown in the Supporting Information. Spectral features in the region below 330 nm reflect the presence of the reduced form of *o*-chloranil and are of little significance.

protection of the OH and NH functions with benzyl and triisopropylsilyl chloride, respectively, prior to reaction with either $\text{Hg}(\text{OAc})_2/\text{I}_2$ in DCM at 0 °C or NIS in THF. This reaction scheme, however, was inapplicable for preparation of unprotected **1a**, since the procedure required for deprotection was not compatible with the iodo substituent. On the other hand, acetylation is by far the most valuable protection strategy in studies of 5,6-dihydroxyindole oxidation, since the free indole can be obtained in situ by mild hydrolysis in phosphate buffer, pH 12, under argon, prior to addition of the oxidant. Accordingly, after several trials, a convenient iodination procedure for 5,6-diacetoxyindole was developed, involving treatment of the substrate with NH_4I , I_2 , and Oxone (3 equiv) in acetonitrile. By this methodology, **1b** was conveniently obtained after a simple workup in fair to good yield (55%) and in sufficiently pure form for subsequent use.

In Situ Generation of **1a** and Oxidation to **1a** Quinone.

Deprotection of **1b** according to the above protocol gave a phenolic product suggestive of **1a** exhibiting a distinct absorption maximum at 300 nm (see the Supporting Information) and migrating on TLC as a single band. All attempts to isolate the

product were unsuccessful, due to the marked instability during workup. Notwithstanding these difficulties,¹⁷ the ^1H and ^{13}C NMR spectra (see the Supporting Information) and the $^1\text{H},^{13}\text{C}$ HSQC and HMBC spectra of the deprotected indole **1a** could be recorded by carefully extracting it into a small volume of AcOEt, adding the organic phase to $\text{DMSO}-d_6$, and fluxing the solution with argon to remove AcOEt. Diagnostic features of the proton spectrum were two apparent singlets at δ 6.59 and 6.80, attributed to the H-4 and H-7 protons and a doublet ($J = 3.0$ Hz) at δ 7.17, due to the H-2 proton. Relative to the unsubstituted 5,6-dihydroxyindole,¹ the iodo substituent at C-3 apparently deshielded the adjacent H-2 proton but caused an upfield shift of the two protons on the benzene moiety. A marked upfield shift of the C-3 carbon signal, resonating at δ 55.8, was observed in the carbon spectrum, showing also CH carbon resonances at δ 127.1, 104.2, and 97.6 which were attributed to the C-2, C-4, and C-7 carbons, in that order, based on heteronuclear 2D experiments. On standing in the NMR tube in $\text{DMSO}-d_6$ for 24 h, **1a** was gradually converted into 5,6-dihydroxyindole (ca. 50% plus other material) as evidenced by both proton and carbon NMR analysis (see the Supporting Information).

Due to the marked instability of **1a**, oxidation experiments were initially carried out by extracting the freshly prepared compound into ethyl acetate and then treating the organic phase in an ice bath with a solution of *o*-chloranil in ethyl acetate. Although this oxidant has a broad absorption maximum at 432 nm, which falls within the expected absorption range of **1a** oxidation products, it proved to be more efficient than other oxidants tested, with little interference caused by its reduced form, tetrachlorocatechol ($\lambda_{\text{max}} = \dots 298$ nm).

Addition of *o*-chloranil (ca. 1 equiv) to an ethyl acetate solution of **1a** in an ice bath caused development of a chromophore with a broad maximum around 400 nm accompanied by another flat, less intense maximum around 600 nm (Figure 1, top trace) which gradually broadened and eventually lost its features after few minutes. None of the features reported correspond to low intensity forbidden transitions of the starting material, as deduced from the starting spectrum of **1a** at the concentration used in the study (see the Supporting Information).

TLC analysis of the reaction mixture in the very first seconds after addition of the oxidant showed complete disappearance of the starting indole. However, rapid addition of aqueous $\text{Na}_2\text{S}_2\text{O}_4$ led to reappearance in the organic phase of a product migrating on TLC as **1a**. To confirm the identity of this latter product, the organic extract was acetylated and analyzed by ^1H NMR, which indicated complete recovery of **1b** with no detectable loss of the halogen. Approximate recovery yield of **1a**, in the form of **1b**, after *o*-chloranil oxidation and $\text{Na}_2\text{S}_2\text{O}_4$ reduction, was 40%. The remainder of the mixture consisted of ill-defined polymeric materials.

For comparison, the same oxidation-reductive quinone-quenching protocol was repeated on 5,6-dihydroxyindole, but all attempts to recover the starting indole met invariably with failure.

Oxidation of **1a** with *o*-chloranil was repeated in phosphate buffer pH 7.0 and resulted in similar chromophoric changes

(15) Tanoue, Y.; Hamada, M.; Kai, N.; Sakata, K.; Hashimoto, M.; Nagai, T. *J. Heterocycl. Chem.* **2005**, *42*, 1195–1199.

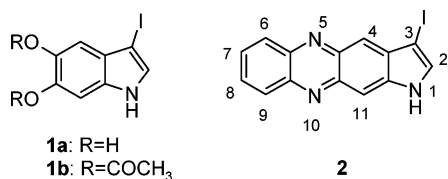
(16) Mee, S. P. H.; Lee, V.; Baldwin, J. E.; Cowley, A. *Tetrahedron* **2004**, *60*, 3695–3712.

(17) One reviewer suggested that anaerobic deprotection of **1b** in an NMR tube in deuterated pH 12 phosphate buffer, followed by neutralization with degassed DCl might furnish nice ^1H and ^{13}C NMR spectra. Unfortunately, this turned out not to be the case, since all attempts were unsuccessful at the concentrations required for running a NMR experiment.

(Figure 1, bottom trace). Overall, these results were consistent with the formation of a relatively long-lived 5,6-indolequinone which survived long enough for spectrophotometric characterization.¹⁸

Despite a careful search of experimental conditions, no meaningful ¹H NMR spectrum of the quinone was obtained: in situ oxidation of **1a** in an NMR tube, for example, gave inconclusive results, because of the rapid degradation of the substrate with formation of dark material apparently polymeric in character. This can be explained considering that the quinone survives at the low concentrations used for the UV spectrum but tends to decompose apparently by polymerization when generated at relatively high concentrations in the NMR tube.

To support formation of the 5,6-indolequinone, freshly prepared **1a** in a cold ethyl acetate solution as above was oxidized with *o*-chloranil and the resulting mixture was immediately treated with a solution of the quinone trapping agent *o*-phenylenediamine in cold ethyl acetate containing acetic acid. TLC analysis revealed the formation of a complex series of products, one of which gave an ESI(+) pseudomolecular ion [M + H]⁺ peak at *m/z* 346, suggesting the expected adduct 3-iodo-1*H*-pyrrolo[2,3-*b*]phenazine (**2**).



Unfortunately, formation yields of the adduct were low, reflecting probably an intrinsically poor reactivity of the 5,6-indolequinone. Nonetheless, the product could be obtained in minute amounts by HPLC purification and was found to exhibit a yellowish chromophore with maxima at 395 and 480 nm (broad). The ¹H NMR spectrum (see the Supporting Information) was consistent with structure **2**, displaying two sets of multiplets around δ 7.9 and 8.2 and three distinct signals at δ 8.08, 8.29, and 8.36. These latter showed one-bond correlation with carbon resonances at δ 139, 118 and 107 and were attributed to the H-2, H-4, and H-7 protons in that order, based on ¹H, ¹³C HSQC and HMBC spectra. Computed carbon resonances determined using the polarizable continuum model (PCM) to model the effects of the solvent showed a satisfactory agreement with experimental values (see the Supporting Information).

Unfortunately, the proposed formulation could not be secured by comparison with an authentic sample due to the complexity of the synthetic goal. To the best of our knowledge, this is the first report describing trapping of a 5,6-indolequinone with *o*-phenylenediamine. Attempts to obtain similar adducts by reaction of the parent 5,6-dihydroxyindole with *o*-phenylenediamine were unsuccessful.

Pulse Radiolysis. Pulse radiolysis was carried out as described previously.^{19,20} Generation of the oxidizing species Br₂^{•-}

(18) Quinones can form charge-transfer complexes (CTC) with hydroquinones, showing typical CTC bands in the visible region (e.g., quinhydrone absorbs at 500–800 nm). CTC formation between **1a** quinone and tetrachlorocatechol is, however, unlikely to be responsible for the UV-vis spectral features in Figure 1 because the spectrum obtained by chemical oxidation is practically the same as obtained by pulse radiolysis (see relevant section below) where no tetrachlorocatechol was present. Further support to this view was provided by oxidation of **1a** by sodium periodate which afforded an UV spectrum similar to that obtained with *o*-chloranil (see the Supporting Information).

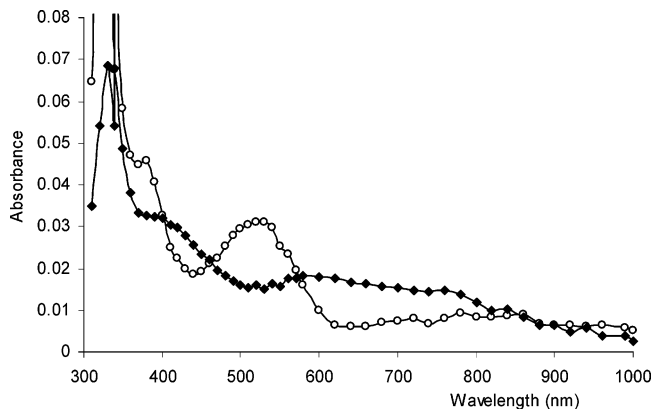
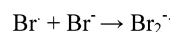
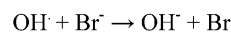
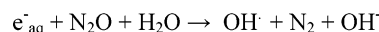
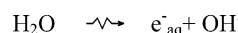


FIGURE 2. Absorbance changes after pulse radiolysis of an N₂O-saturated aqueous solution of **1a** (1.5×10^{-4} M) in 0.5 M KBr/7.0 $\times 10^{-2}$ M phosphate buffer, pH 7.0: (○) 18 μ s; (◆) 874 μ s.

was achieved by irradiating N₂O-saturated solutions of 0.5 M KBr, and Br₂^{•-} radicals are formed within 0.1 μ s after the radiation pulse according to the following equations.



Compound **1a** was obtained in situ by an efficient deacetylation procedure compatible with the experimental conditions for pulse radiolysis, involving treatment of the acetylated indole under a N₂O atmosphere with 0.025 M trisodium phosphate containing 0.5 M KBr, followed by addition of sodium dihydrogen phosphate to pH 7.0. Compound **1a** thus prepared (0.15 mM) was subjected to pulse radiolysis and the transient absorption spectra are shown in Figure 2 (for a complete series of absorption spectra see the Supporting Information).

The first transient spectrum was recorded at such a time that the buildup of initial radical absorption was complete and that subsequent decay had not proceeded to any significant extent. The chromophore appearing 18 μ s after the pulse displayed a shoulder at 380 nm and a maximum at 520 nm and was attributed to 5,6-dihydroxy-3-iodoindole semiquinone. The iodo substituent apparently shifts the low energy transitions of 5,6-dihydroxyindole semiquinone by 20–30 nm.¹¹ The rate constant for the reaction of **1a** with Br₂^{•-} was estimated to be $k = 2.2 \times 10^9 \text{ M}^{-1} \text{ s}^{-1}$. The extinction coefficient of the semiquinone at 520 nm was calculated to be $2300 \text{ M}^{-1} \text{ cm}^{-1}$, close to that of the corresponding semiquinone of the parent 5,6-dihydroxyindole.¹¹ Oxygen-centered semiquinone radicals from 5,6-dihydroxyindoles usually disproportionate to give 5,6-indolequinones and reform 5,6-dihydroxyindoles by a second-order process,¹¹ so it could be anticipated that the semiquinone from **1a** behaves similarly in undergoing disproportionation to produce an indolequinone species. However, close scrutiny of the pulse radiolysis data indicated a semiquinone decay rate much faster

(19) Napolitano, A.; Di Donato, P.; Prota, G.; Land, E. J. *Free Radic. Biol. Med.* **1999**, *27*, 521–528.

(20) Land, E. J.; Ramsden, C. A.; Riley, P. A. *J. Photochem. Photobiol. B* **2001**, *64*, 123–135.

than those of most semiquinones so far investigated,^{19–21} and indeed, from the second-order plot a disproportionation rate constant $2k = 1.1 \times 10^{10} \text{ M}^{-1} \text{ s}^{-1}$ was determined. The spectrum detected after 136 μs and at longer times after the pulse (Figure 2 and spectra in the Supporting Information) displayed a shoulder around 400 nm and broad flattened bands centered around 600 and 750 nm, resembling the absorption features of the putative 5,6-indolequinone(s),¹¹ and was likely due to a quinone species. This chromophore bears considerable resemblance to that of the species produced by oxidation of **1a** with *o*-chloranil in both organic solvent and aqueous buffer (Figure 1), supporting the view that in those experiments *o*-chloranil-derived species are not responsible for the transient absorption spectrum.

Monitoring spectral changes in the 350–560 nm region and above 850 nm showed that approximately 40% of the absorption at 440 nm had decayed after 1 s, indicating that this quinone species is relatively long-lived. However, monitoring in the region 560–680 nm a growth is noted over about 10 ms which at 620 nm has a first-order rate constant of $9.6 \times 10^2 \text{ s}^{-1}$, as deduced from data in the plot shown in the Supporting Information, and is not much changed on lowering the dose.

Overall, these data may be interpreted to suggest partial tautomerism between the first-formed quinone species.

DFT Calculations. To aid in the identification of the main species produced during **1a** oxidation, the parent indole and putative semiquinone and quinone intermediates in the process were geometry-optimized in vacuo at the PBE0/6-31+G(d,p) level of theory.^{22,23} To account for the influence of the aqueous environment, all structures were also optimized using the PCM model²⁴ in its united atom for Hartree–Fock (UAHF) parametrization.²⁵ Computational output for the starting material, intermediates and their tautomeric forms (geometries and energies) is reported in the Supporting Information. The absorption spectra of all species that were within 10 kcal mol⁻¹ from the corresponding lowest-energy structure were simulated both in vacuo and in water at the TD-DFT level,²⁶ using the large 6-311+G(2d,2p) basis set. The computational levels chosen have been validated in a number of previous studies, in particular for what concerns energies and geometries²⁷ and low-lying electronic transitions.²⁸

Ionization equilibria were considered for **1a** semiquinones, assuming that $\text{p}K_{\text{a}}$ values are not too different from those of other related semiquinones. The $\text{p}K_{\text{a}}$ values for the 6-OH groups of the semiquinones derived from both 5,6-dihydroxyindole and *N*-methyl-5,6-dihydroxyindole have been reported to be 6.8.²⁹ The $\text{p}K_{\text{a}}$ values for the semiquinones from 2-methyl- and 2,3-

dimethyl-5,6-dihydroxyindole were determined to be 6.6 and 6.3, respectively.³⁰ This suggests that the first formed semiquinone may be present at least in part in the ionized form.

DFT analysis was carried out for the possible isomers of both neutral and ionized semiquinone radicals (Scheme 2). Data predicted the 6-OH-derived phenoxyl radical (**I**) as the favored neutral species both in vacuo and in water, though the 5-OH-derived radical **II** is destabilized by only 0.9–1.1 kcal mol⁻¹. The NH-derived radical tautomer (**III**) is the least stable. Like the OH-derived radicals, this latter radical is π in character, a feature that in this case implies substantial loss of aromaticity. Moreover, a stronger intramolecular O–H \cdots O bond is possible for the *O*-centered radicals than for the *N*-centered species (see the Supporting Information).

The relative stability of the *O*-centered radicals can be rationalized considering that in **I**, but not in **II**, the odd electron may be efficiently delocalized to the pyrrole ring, as can be appreciated from inspection of resonance structures. While solvation effects alter the relative energy separation of the tautomers, the same order of stability is preserved in vacuo and in water (see the Supporting Information). Among the anion forms, the *N*-protonated species **IV** was the most stable, with the *O*-5 protonated species (**V**) being only 1.4 kcal mol⁻¹ higher in energy in water. Again, the possibility of a larger delocalization of the unpaired electron or the negative charge from the oxygen at C-6 dictated the relative stability of the ionized radicals.

Figure 3 shows the computed absorption spectra of neutral and anion forms of the semiquinone over the wavelength region of interest both in vacuo and in water. Interestingly, the most stable neutral form, viz. the 6-*O* phenoxyl radical **I** exhibits distinct electronic transitions around 300, 350 (sh), and 500 nm in water. The band at 500 nm was lacked by the other neutral forms as well as by the most stable *N*-protonated anion. However, the *O*-5 protonated semiquinone anion **V**, accounting for some 20% of the semiquinone anion equilibrium mixture based on relative energies, also displays an intense absorption at 500 nm. The calculated spectrum of the most stable anion form of the semiquinone (**IV**) revealed distinct transitions at 310 and 360 (sh) nm. Thus, it appears that both the neutral and anion forms of the semiquinone can contribute as expected to the chromophore that develops following one-electron oxidation of **1a**.

Three main tautomers were considered for the two-electron oxidation product, namely the *o*-quinone, the quinone–methide, and the quinonimine forms.

(21) Lambert, C.; Land, E. J.; Riley, P. A.; Truscott, G. T. *Biochim. Biophys. Acta* **1990**, *1035*, 319–324.

(22) Adamo, C.; Barone, V. *J. Chem. Phys.* **1999**, *110*, 6158–6170.

(23) Francl, M. M.; Petro, W. J.; Hehre, W. J. S.; Binkley, J.; Gordon, M. S.; DeFrees, D. J.; Pople, J. A. *J. Chem. Phys.* **1982**, *77*, 3654–3665. For a general introduction to basis sets, see: Foresman, J. B.; Frisch, A. *Exploring Chemistry with Electronic Structure Methods*, 2nd ed.; Gaussian, Inc.: Pittsburgh, PA, 1996.

(24) (a) Miertus, S.; Scrocco, E.; Tomasi, J. *J. Chem. Phys.* **1981**, *55*, 117–129. (b) Cossi, M.; Scalmani, G.; Rega, N.; Barone, V. *J. Chem. Phys.* **2002**, *117*, 43–54. (c) Scalmani, G.; Barone, V.; Kudin, K. N.; Pomelli, C. S.; Scuseria, G. E.; Frisch, M. J. *Theor. Chem. Acc.* **2004**, *111*, 90–100.

(25) Barone, V.; Cossi, M.; Tomasi, J. *J. Chem. Phys.* **1997**, *107*, 3210–3221.

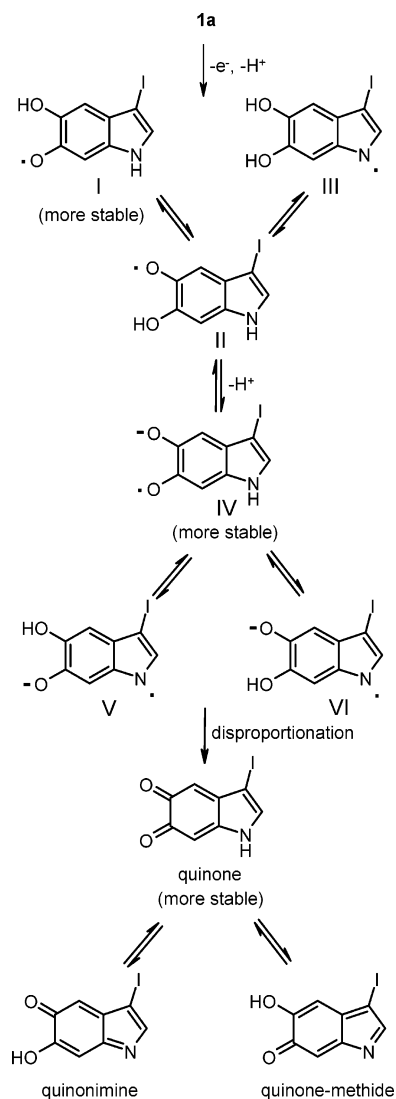
(26) (a) Stratmann, R. E.; Scuseria, G. E.; Frisch, M. J. *J. Chem. Phys.* **1998**, *109*, 8218–8224. (b) Bauernschmitt, R.; Ahlrichs, R. *Chem. Phys. Lett.* **1996**, *256*, 454–464. (c) Casida, M. E.; Jamorski, C.; Casida, K. C.; Salahub, D. R. *J. Chem. Phys.* **1998**, *108*, 4439–4449. (d) Adamo, C.; Scuseria, G. E.; Barone, V. *J. Chem. Phys.* **1999**, *111*, 2889–2899.

(27) (a) Improta, R.; Barone, V. *J. Am. Chem. Soc.* **2004**, *126*, 14320–14321. (b) Benzi, C.; Improta, R.; Scalmani, G.; Barone, V. *J. Comput. Chem.* **2002**, *23*, 341–350. (c) Langella, E.; Rega, N.; Improta, R.; Crescenzi, O.; Barone, V. *J. Comput. Chem.* **2002**, *23*, 650–661. (d) Improta, R.; Mele, F.; Crescenzi, O.; Benzi, C.; Barone, V. *J. Am. Chem. Soc.* **2002**, *124*, 7857–7865.

(28) (a) Jacquemin, D.; Wathelet, V.; Perpète, E. A. *J. Phys. Chem. A* **2006**, *110*, 9145–9152. (b) Preat, J.; Jacquemin, D.; Wathelet, V.; Andre, J.-M.; Perpète, E. A. *J. Phys. Chem. A* **2006**, *110*, 8144–8150. (c) Jacquemin, D.; Preat, J.; Wathelet, V.; Fontaine, M.; Perpète, E. A. *J. Am. Chem. Soc.* **2006**, *128*, 2072–2083. (d) Crescenzi, O.; Pavone, M.; De Angelis, F.; Barone, V. *J. Phys. Chem. B* **2005**, *109*, 445–453. (e) Aquilante, F.; Cossi, M.; Crescenzi, O.; Scalmani, G.; Barone, V. *Mol. Phys.* **2003**, *101*, 1945–1953. (f) Adamo, C.; Barone, V. *Chem. Phys. Lett.* **2000**, *330*, 152–160.

(29) Al-Kazwini, A. T.; O'Neill, P.; Adams, G. E.; Cundall, R. B.; Jacquet, B.; Lang, G.; Junino, A. *J. Phys. Chem.* **1990**, *94*, 6666–6670.

(30) Al-Kazwini, A. T.; O'Neill, P.; Adams, G. E.; Cundall, R. B.; Maignan, J.; Junino, B. *Melanoma Res.* **1994**, *4*, 343–350.

SCHEME 2 Overall View of the Possible Intermediates Arising by Oxidation of 1a^a


^a Valence structures shown do not reflect actual charge and spin density distributions. Highlighted are relatively more stable species as predicted by DFT-PCM.

Structure energy data indicated that in vacuo the quinone-methide is favored over the *o*-quinone by ca. 2.8 kcal mol⁻¹, due to the a strong (ca. 7 kcal mol⁻¹) intramolecular OH-O hydrogen bond. However, solvation stabilizes the *o*-quinone significantly more than the quinone-methide, so that in water the relative energy of the latter with respect to the *o*-quinone is ca. 6.0 kcal mol⁻¹ (see the Supporting Information). The relative stability of the parent 5,6-indolequinone tautomers and the underlying factors have been addressed in a previous study,² showing that the *o*-quinone is the favored species *both* in water and in vacuo, though in the latter case the energy of the quinone-methide was predicted to be very close, entailing that 4–25% of 5,6-indolequinone would exist in the gas phase as quinone-methide. The present results would therefore indicate that in vacuo the 3-iodo substituent further stabilizes the quinone-methide relative to the *o*-quinone. Both in vacuo and in water, the quinonimine is relatively unstable (>6.2 kcal mol⁻¹) and is therefore unlikely to contribute to the measured

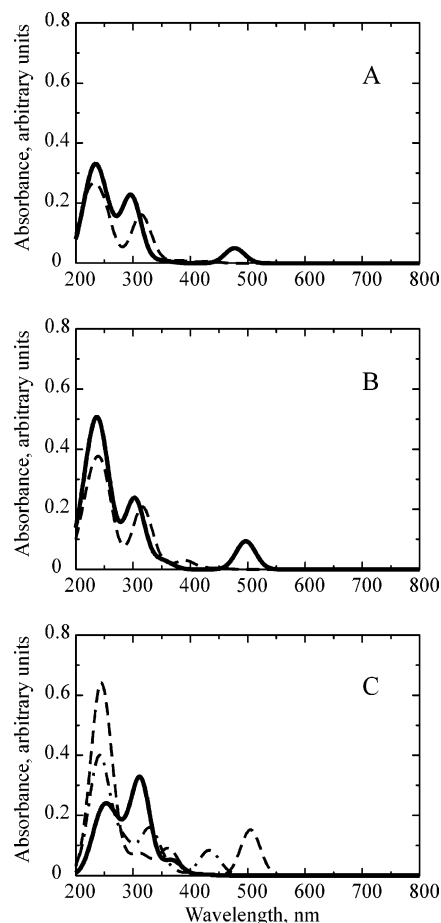


FIGURE 3. UV-vis spectra of 5,6-dihydroxy-3-iodoindole semi-quinones computed at the PBE0/6-311+G(2d,2p)/PBE0/6-31+G(d,p) level. Panel A, neutral forms in vacuo: solid line, 6-*O* radical (**I**); dashed line, 5-*O* radical (**II**) (relative energy 0.9 kcal mol⁻¹). Panel B, neutral forms in aqueous solution (PCM): solid line, 6-*O* radical (**I**); dashed line, 5-*O* radical (**II**) (1.1 kcal mol⁻¹). Panel C, anionic forms in aqueous solution (PCM): solid line, *N*-protonated form (**IV**); dashed, 5-*O*-protonated form (**V**) (1.4 kcal mol⁻¹); dashed-dotted line, 6-*O*-protonated form (**VI**) (3.8 kcal mol⁻¹). In each case, the spectrum of the most stable reference component is highlighted in bold.

absorption spectrum for the putative quinone. Computed absorption spectra of all the quinone tautomers are reported in Figure 4.

The data show that in vacuo the most stable quinone-methide structure exhibits significant absorption around 380 nm accompanied by a second broad, less intense maximum around 710 nm. The calculated spectrum of this tautomer is not much affected by the medium and is in satisfactory agreement with the spectrum of the species produced by oxidation of the indole with *o*-chloranil in ethyl acetate. Calculated absorption features of the *o*-quinone in water comprise two weak low energy transitions around 400 and 820 nm while at lower wavelengths an intense band at 270 nm is present. In vacuo, a blue shift of the chromophore is observed, with main bands at 250, 366 and 645 nm. When this information is used to determine the identity of the putative quinonoid species formed by oxidation of **1a**, supporting evidence in favor of the indolequinone structure is obtained, though a comment seems in order here.

As mentioned earlier, the marked analogy of the chromophore produced by disproportionation of the pulse radiolytically generated semiquinone with that of the species generated by

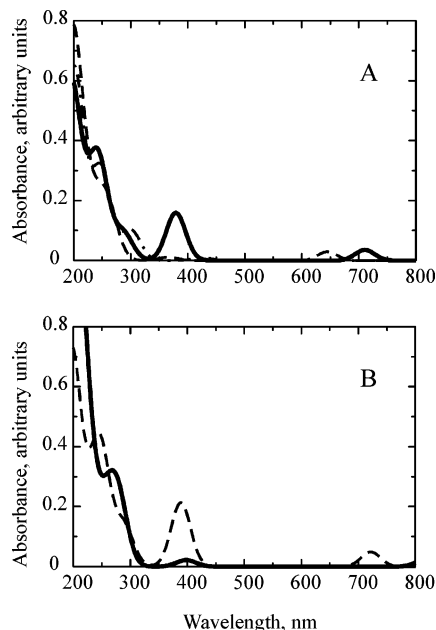


FIGURE 4. UV-vis spectra of 5,6-dihydroxy-3-iodoindole quinone tautomers, computed at the PBE0/6-311+G(2d,2p)//PBE0/6-31+G(d,p) level. Panel A, in vacuo: full line, quinone-methide; dashed line, quinone (relative energy 2.8 kcal mol⁻¹); dashed-dotted line, quinonimine (6.2 kcal mol⁻¹). Panel B, aqueous solution (PCM): full line, quinone; dashed line, quinone-methide (6.0 kcal mol⁻¹); during optimization in aqueous solution, the quinonimine tautomer (in its hydrogen-bonded form) converted to the quinone-methide. In each case, the spectrum of the most stable, reference component is highlighted in bold.

o-chloranil oxidation of **1a** in both ethyl acetate and aqueous buffer may be taken to indicate either that similar species are produced in both media, or that different species or mixtures of species are formed, but with similar chromophores. Computational analysis suggests that this latter might indeed be the case. Comparison of the computed absorption spectra of the *o*-quinone and quinone-methide tautomers both in vacuo and in water indicates that the former is much more solvent-sensitive, as noted above, and that both species display absorptions in the regions near 400 nm and above 600 nm. However, whereas there is a general superimposition of bands around 400 nm for the two tautomers, more pronounced differences are observed in the low energy transitions though data should be used with caution given the potential inaccuracy of transitions computed at these low energies. The rather poor features of the experimental spectra for the putative quinones obtained in ethyl acetate and in water would not rule out the possibility that a mixture of tautomers is actually formed, on account of the first-order process observed after semiquinone decay in the pulse radiolysis experiments. Calculated spectra for **1a** quinone anion (all tautomers of the quinone form the same anion) did not reveal any appreciable absorption in the 400–1000 nm region (see SI) suggesting that ionized quinone does not contribute appreciably to the high wavelength absorption. Another possibility is that **1a** quinone in its pure form absorbs mainly at ~400 nm as predicted, whereas the observed features in the long wavelength region arise mainly from a charge-transfer complex (CTC) between quinone and catechol species. Though the fraction of **1a** which undergoes oxidation during pulse radiolysis is minimal and, moreover, disproportionation of **1a**–semiquinone also regenerates equimolar amounts of **1a** and its

quinone, a CTC mechanism between these two species may in principle contribute to the transient absorption spectrum in Figure 2, especially for what concerns the long wavelength region. However, the low concentrations achieved in the pulse radiolysis experiments would not support this possibility. As a matter of fact, it is known that quinhydrone-type systems are not very soluble and dissociate considerably to their components in solution.³¹ CTC formation between 5,6-dihydroxyindoles and their quinones is an interesting issue to be addressed in future studies.

As far as the nature of the transitions underlying the UV-vis spectrum is concerned, the π - π^* transition at 710 nm (oscillator strength, $f = 0.036$) in the 3-iodoindolequinone-methide spectrum (in vacuo) is HOMO-LUMO in character (see the Supporting Information) and is paralleled by a corresponding transition in the 3-unsubstituted quinone-methide (702 nm, $f = 0.018$, see also previous work²). However, the 380 nm transition of the iodinated methide ($f = 0.159$), which is essentially HOMO-1-LUMO in character, involves excitation from an iodine p-orbital and has clearly no counterpart in the parent methide. The situation is rather similar for the *o*-quinone tautomers: the longest wavelength allowed bands are HOMO-LUMO in character and quite similar in the 3-iodo compound and in the unsubstituted quinone (645 nm, $f = 0.029$, and 610 nm, $f = 0.033$, respectively), while the 366 nm transition ($f = 0.011$, HOMO-2 - LUMO in this case) is present only for the iodinated quinone as it involves strong participation of a p orbital on the iodine atom.

This conclusion does not help settle the 5,6-indolequinone chromophore conundrum, but allows us to demonstrate that there is a significant difference in the absorption spectra of 5,6-indolequinone and its 3-iodo derivative, and that the spectroscopic features of the latter are in much better agreement with the theoretical predictions. An overall view of the species computed in this study and their mutual relationships is provided in Scheme 2.

Conclusions

In summary, we have described the labile semiquinone and quinone species produced by oxidation of 5,6-dihydroxy-3-iodoindole (**1a**). Realization of this goal was made possible by introduction of the iodo substituent on the 3-position of the indole ring, which increased the lifetime of 5,6-indolequinone enough to permit registration of the electronic absorption spectrum and to allow for partial trapping with *o*-phenylenediamine. Pulse radiolytic investigations revealed the generation of one or more transient radical or radical-anion forms of the semiquinone which rapidly disproportionates to give the *o*-indolequinone. Computational analysis at the DFT level of theory suggested medium-dependent tautomerism in quinone species, with the *o*-quinone prevailing in aqueous medium and the quinone-methide in less polar organic solvents. The strong participation of a p orbital on the iodine atom in the 360–380 nm transitions predicted for the *o*-quinone and quinone-methide tautomers is another highlight from this study. Overall, these results provide an additional contribution toward the elucidation

(31) (a) Berthoud, A.; Kunz, S. *Helv. Chim. Acta* **1938**, *21*, 17–22. (b) Tsubomura, H. *Bull. Chem. Soc. Jpn.* **1953**, *26*, 304–311. (c) Kuboyama, A.; Nagakura, S. *J. Am. Chem. Soc.* **1955**, *77*, 2644–2646. (d) Moser, R. E.; Cassidy, H. G. *J. Am. Chem. Soc.* **1965**, *87*, 3463–3467. (e) Calderazzo, F.; Forte, C.; Marchetti, F.; Pampaloni, G.; Pieretti, L. *Helv. Chim. Acta* **2004**, *87*, 781–789.

of the structure and chemical properties of 5,6-indolequinones and underscore the investigative potential of the combined chemical, pulse radiolytic and quantum mechanical approach reported in the present study.

Experimental Section

5,6-Dihydroxyindole³² and 5,6-diacetoxyindole³³ were synthesized as previously reported. For general experimental methods and other materials, see the Supporting Information.

Preparation of 5,6-Diacetoxy-3-iodoindole (1b). A general procedure reported in the literature³⁴ was adopted with modifications. Briefly, Oxone (11.9 g, 19.2 mmol) was added to a stirred solution of NH₄I (1.4 g, 9.6 mmol), I₂ (2.4 g, 9.6 mmol), and 5,6-diacetoxyindole (1.5 g, 6.4 mmol) in acetonitrile (30 mL), and the reaction mixture was taken under stirring at room temperature. After 1 h, at complete substrate consumption (TLC evidence, *R_f* 0.62 eluant CHCl₃/CH₃OH 9:1), the reaction mixture was diluted with ethyl acetate (60 mL) and washed with a 0.1% Na₂S₂O₃/1% NaCl solution (2 × 50 mL) and then with water (2 × 50 mL). The combined organic layers were dried over sodium sulfate, and the solvent was removed under reduced pressure. The resulting dark oil was purified by column chromatography (eluant CHCl₃) to give **1b** (1.27 g; 55% yield, *R_f* 0.68 (CHCl₃/MeOH, 9:1, > 98% purity) as a yellow solid. Crystallization from ethanol gave colorless needles, decomposing over 110 °C.

1b: UV (MeOH) λ_{max} 284, 292 (sh) nm; IR (CCl₄) ν_{max} 3479, 3395, 1770, 1468, 1370, 1326, 1232, 1116, 1009, 920, 871 cm⁻¹; ¹H NMR (acetone-*d*₆) δ 2.28 (3H, s), 2.29 (3H, s), 7.17 (1H, s, H-4), 7.36 (1H, s, H-7), 7.56 (1H, d, *J* = 3.0 Hz, H-2), 10.88 (1H, bs, NH); ¹³C NMR (acetone-*d*₆) 20.0 (2 × CH₃), 54.2 (C-3), 106.2 (C-7), 113.6 (C-4), 127.4 (C-9), 131.2 (C-2), 133.0 (C-8), 137.5 (C-5), 139.4 (C-6), 168.3 (CO), 168.6 (CO); ¹H and ¹³C NMR spectra are provided as Supporting Information; ESI+/MS *m/z* 360 [M + H]⁺, 382 [M + Na]⁺, 719 [2M + H]⁺, 741 [2M + Na]⁺; HR ESI+/MS found 359.9730 ([M + H]⁺), calcd for C₁₂H₁₀NO₄I *m/z* 359.9733.

Preparation of 5,6-Dihydroxy-3-iodoindole (1a). A solution of **1b** (5 mg, 0.014 mmol) in methanol (1.0 mL) was slowly added under vigorous stirring to a 0.025 M trisodium phosphate solution (2.5 mL) that had previously been purged with argon. The reaction mixture was stirred under an argon atmosphere and after 10 min acidified to pH 4 with 2 M HCl, and the mixture was extracted with ethyl acetate (2 × 2.5 mL). Note that the solutions of **1a** in ethyl acetate are highly unstable and cannot be taken to dryness even in the cold. For NMR analysis of **1a** the reaction was carried out on 5 (or 50) mg of **1b** in 0.025 M trisodium phosphate solution (1 (or 50) mL) and the ethyl acetate extract (1 (or 3 × 50) mL) was added to acetone-*d*₆ (5 mL) or DMSO-*d*₆ (600 μL), in this case the ethyl acetate was removed by fluxing the solution with anhydrous argon).

1a: UV λ_{max} (pH 7.0) 300 nm; ¹H NMR (acetone-*d*₆) δ 6.71 (1H, s, H-4), 6.87 (1H, s, H-7), 7.28 (1H, d, *J* = 3.0 Hz, H-2); ¹H NMR (DMSO-*d*₆) δ 6.59 (1H, s, H-4), 6.80 (1H, s, H-7), 7.17 (1H, bs, H-2), 8.66, 8.77 (bs, OH), 10.87 (1H, bs, NH); ¹³C NMR (DMSO-*d*₆) δ 55.8 (C-3), 97.6 (C-7), 104.2 (C-4), 122.4 (C-9), 127.1 (C-2), 130.0 (C-8), 141.8 (C-5), 143.9 (C-6); ¹H and ¹³C NMR spectra are provided as Supporting Information; ESI+/MS *m/z* 276 [M + H]⁺, 298 [M + Na]⁺, 573 [2M + Na]⁺.

Chemical Oxidation of 1a. All of the following experiments were performed on ice-bath cooled solutions and solvents. For the spectrophotometric experiments, an aliquot (100 μL) of the solution of **1a** obtained as described above was diluted with ethyl acetate

(2.9 mL) in a cuvette thermostated by circulation of ice-cold water and treated under stirring with 110 μL of a 2.5 mM solution of *o*-chloranil in ethyl acetate. Absorption spectra were immediately recorded by a diode array spectrophotometer over 1 min period at 15 s time intervals. In other experiments, the phosphate solution containing **1a** was taken to pH 7 with 2 M HCl. An aliquot of the solution (50 μL) was diluted with cold 50 mM phosphate buffer pH 7.0 (2.9 mL) and treated under the conditions described above with 110 μL of a solution of *o*-chloranil in methanol. When necessary the oxidation mixtures at 15 s were analyzed by HPLC (eluant as for LC/MS analysis) to estimate residual chloranil. Experiments using sodium periodate were run under the conditions described above in phosphate buffer pH 6.0 with addition of the oxidant in water.

In other experiments, the solution of **1a** in ethyl acetate obtained as described above but starting from 20 mg of **1b** was oxidized with an equimolar solution of *o*-chloranil in ethyl acetate. After 20 s, the organic layer was washed with a 1% Na₂S₂O₄ solution (5 mL) and then directly treated with an equal volume of acetic anhydride containing 5% pyridine overnight at rt. After removal of the volatile components the residue was analyzed by TLC and was found to consist mainly of **1b** which was purified by preparative TLC (8 mg, *R_f* 0.68 (CHCl₃/MeOH, 9:1)).

Isolation of 3-Iodo-1*H*-pyrrolo[2,3-*b*]phenazine (2). To a solution of **1a** in ethyl acetate prepared as described above from 50 mg of **1b** taken in an ice bath was added a cooled solution of *o*-chloranil (69 mg, 0.28 mmol) in ethyl acetate (6.7 mL). After 30 s, the reaction mixture was added to 16 mL of glacial acetic acid at rt, followed by a solution of *o*-phenylenediamine (76 mg, 0.70 mmol) in ethyl acetate (6.7 mL). After 2 min, the reaction mixture was washed with water (40 mL), dried over sodium sulfate and taken to dryness to give a brown residue. This was dissolved in ethyl acetate and analyzed by LC/ESI+MS. Preparative TLC fractionation (eluant CHCl₃/CH₃OH 9:1 v/v) gave a band at *R_f* 0.47 (5 mg) that was further purified by semipreparative HPLC (eluant 0.1% TFA/acetonitrile 1:1 v/v) to give **2** (*t_R* 46 min, 1 mg, 80% purity): UV λ_{max} (CH₃OH) 244, 280, 395, 483 (b) nm; ¹H NMR (acetone-*d*₆) δ 7.86 (2H, m, H-7, H-8), 8.08 (1H, br s, H-2), 8.21–8.25 (2H, m, H-6, H-9), 8.28 (1H, s, H-4), 8.35 (1H, s, H-7); ¹³C NMR (acetone-*d*₆) δ 55 (C-3), 107 (C-11), 118 (C-4), 128 (C-6/C-9), 129 (C-7/C-8), 136–139 (C-3a/C-4a), 139 (C-2), 139–141 (C-10a/C-11a); (LC-ESI+/MS *t_R* 27.5 min, *m/z* 346 ([M + H]⁺); HR ESI+/MS found 345.9872 ([M + H]⁺), calcd for C₁₄H₉N₃I *m/z* 345.9841.

Pulse Radiolysis. The pulse radiolysis experiments were performed with the 12 MeV linear accelerator at the Daresbury Laboratory, using the Free Radical Research Facility.³⁵ This accelerator provides pulse lengths of between 0.2 and 2 μs with doses up to 30 Gy using quartz capillary cells of optical path 2.5 cm. Absorbed doses were determined from the transient (CNS)₂⁻ formation in air-saturated potassium thiocyanate solutions (10 mM) using a G of 0.30 μM/Gy and ε (500 nm) = 7100 M⁻¹ cm⁻¹.³⁶ The estimates of the molar absorption coefficients and rate constants are considered to be correct to ±15%. In a typical experiment, a solution of **1b** in methanol (15 mM) was treated under a N₂O atmosphere with a solution of 0.025 M trisodium phosphate containing 0.5 M KBr up to a 0.15 mM concentration, and after 10 min the pH of the solution was taken to 7.0 by addition of NaH₂

(35) (a) Butler, J.; Hodgson, B. W.; Hoey, B. M.; Land, E. J.; Lea, J. S.; Lindley, E. J.; Rushton, F. A. P.; Swallow, A. J. *Radiat. Phys. Chem.* **1989**, *34*, 633–646. (b) Holder, D. J.; Allan, D.; Land, E. J.; Navaratnam, S. In *Proceedings of the 8th European Particle Accelerator Conference*; Garvey, T., Le Duff, J., Le Roux, P., Petit-Jean-Genaz, C., Poole, J., Rivki, L., Eds.; European Physical Society: Paris, 2002; pp 2804–2806.

(36) (a) Buxton, G. V.; Stuart, C. R. *J. Chem. Soc., Faraday Trans.* **1995**, *91*, 279–281. (b) Adams, G. E.; Boag, J. W.; Currant, J.; Michael, B. D. In *Pulse Radiolysis*; Ebert, M., Keene, J. P., Swallow, A. J., Baxendale, J. H., Eds.; Academic Press: London, 1965; pp 117–129.

(32) Benigni J. D.; Minnis, R. L. *J. Heterocycl. Chem.* **1965**, *2*, 387–392.

(33) Murphy, B. P. *J. Org. Chem.* **1985**, *50*, 5873–5875.

(34) Krishna Mohan, K. V. V.; Narender, N.; Kulkarni, S. J. *Tetrahedron Lett.* **2004**, *45*, 8015–8018.

PO₄ (0.07 M final concentration of phosphate buffer). The resulting mixture was subjected to pulse radiolysis.

Computational Methods. All calculations were performed with the Gaussian 03 package of programs.³⁷ Geometries were optimized at the DFT level of theory using the PBE0 functional with the 6-31+G(d,p) basis set.^{22,23} For the iodine atom, a valence basis with pseudopotentials was employed,³⁸ augmented with one d function.³⁹ The PBE0²² (also referred to as PBE1PBE) is a hybrid functional obtained by combining a predetermined amount of exact exchange with the Perdew–Burke–Ernzerhof exchange and correlation functionals.⁴⁰ To simulate the aqueous environment, the polarizable continuum model (PCM)²⁴ was used, in combination with the UAHF parametrization for atomic radii.²⁵ All minima were checked by frequency calculation. Electronic absorption spectra of significant tautomers were estimated on the basis of excitation energy calculations using the TDDFT approach.²⁶ The PBE0 functional with the large 6-311+G(2d,2p) basis set were used for TDDFT computations, and a second d function was added on the iodine atom.³⁹ Spectra in solution were computed with the non-equilibrium formulation of the PCM method.⁴¹ To produce graphs of computed UV–vis spectra, transitions above 190 nm were selected, and an arbitrary Gaussian line width of 20 nm was imposed. NMR shielding constants were computed with the gauge-

including atomic orbitals (GIAO) approach²⁶ in combination with the 6-311+G(d,p) basis set and were converted into chemical shift by referencing to the shieldings of a standard compound (benzene) computed at the same level.

Acknowledgment. This work was carried out in the frame of the project “An integrated approach to the synthesis characterization and functions of 5,6-dihydroxyindole-derived eumelanin biopolymer and their blending with conventional polymers and composites” supported by MIUR (PRIN 2006). We thank the CampusGrid of the University Federico II of Naples for computational resources. The pulse radiolysis experiments were carried out at the Free Radical Research Facility (Station 0.1) in the Synchrotron Radiation Department of the CCLRC Daresbury Laboratory, Warrington, U.K., in the frame of the project no. AP46154. We thank the “Centro Interdipartimentale di Metodologie Chimico-Fisiche” (CIMCF, University of Naples Federico II) for NMR and mass spectrometry facilities. The technical assistance of Mrs. Silvana Corsani is gratefully acknowledged.

Supporting Information Available: General methods; ¹H NMR spectral data for compound **1a,b** and **2**; ¹³C NMR spectral data for compounds **1a,b**; ¹H, ¹³C DEPT HSQC and ¹H, ¹³C HMBC spectra of **2**; experimental vs calculated ¹³C resonances of compound **2**; UV spectrum of compound **1a**, spectral time monitoring for the conversion of **1a** to 5,6-dihydroxyindole, and hydrolysis of **1b**; UV spectra of chemical oxidation of **1a**; spectra of the pulse radiolytic oxidation of **1a** at different times; time profile of the transmission changes during pulse radiolytic oxidation of **1a** at different wavelengths; coordinates (Å), absolute energies (hartrees), and relative energies of tautomers/conformers/ionization states of **1a**, its quinone and semiquinone; isodensity surfaces of molecular orbitals underlying the long-wavelength allowed transitions of 3-iodoindolequinone and indolequinone; computed UV–vis spectra of **1a**-semiquinone, methide, and their anionic forms; computed energies of tautomers/conformers of 5,6-dihydroxy-3-iodoindole-semiquinone and 3-iodo-5,6-indolequinone in vacuo and in aqueous solution (PCM). This material is available free of charge via the Internet at <http://pubs.acs.org>.

JO0615807

(37) Frisch, M. J.; Trucks, G. W.; Schlegel, H. B.; Scuseria, G. E.; Robb, M. A.; Cheeseman, J. R.; Montgomery, J. A., Jr.; Vreven, T.; Kudin, K. N.; Burant, J. C.; Millam, J. M.; Iyengar, S. S.; Tomasi, J.; Barone, V.; Mennucci, B.; Cossi, M.; Scalmani, G.; Rega, N.; Petersson, G. A.; Nakatsuji, H.; Hada, M.; Ehara, M.; Toyota, K.; Fukuda, R.; Hasegawa, J.; Ishida, M.; Nakajima, T.; Honda, Y.; Kitao, O.; Nakai, H.; Klene, M.; Li, X.; Knox, J. E.; Hratchian, H. P.; Cross, J. B.; Bakken, V.; Adamo, C.; Jaramillo, J.; Gomperts, R.; Stratmann, R. E.; Yazyev, O.; Austin, A. J.; Cammi, R.; Pomelli, C.; Ochterski, J. W.; Ayala, P. Y.; Morokuma, K.; Voth, G. A.; Salvador, P.; Dannenberg, J. J.; Zakrzewski, V. G.; Dapprich, S.; Daniels, A. D.; Strain, M. C.; Farkas, O.; Malick, D. K.; Rabuck, A. D.; Raghavachari, K.; Foresman, J. B.; Ortiz, J. V.; Cui, Q.; Baboul, A. G.; Clifford, S.; Cioslowski, J.; Stefanov, B. B.; Liu, G.; Liashenko, A.; Piskorz, P.; Komaromi, I.; Martin, R. L.; Fox, D. J.; Keith, T.; Al-Laham, M. A.; Peng, C. Y.; Nanayakkara, A.; Challacombe, M.; Gill, P. M. W.; Johnson, B.; Chen, W.; Wong, M. W.; Gonzalez, C.; Pople, J. A. *Gaussian 03*, Revision C.02; Gaussian, Inc.: Wallingford, CT, 2004.

(38) Bergner, A.; Dolg, M.; Kuechle, W.; Stoll, H.; Preuss, H. *Mol. Phys.* **1993**, *80*, 1431–1441.

(39) Peterson, K. A.; Figgen, D.; Goll, E.; Stoll, H.; Dolg, M. *J. Chem. Phys.* **2003**, *119*, 11113–11123.

(40) (a) Perdew, J. P.; Burke, K.; Ernzerhof, M. *Phys. Rev. Lett.* **1996**, *77*, 3865–3868. (b) Perdew, J. P.; Burke, K.; Ernzerhof, M. *Phys. Rev. Lett.* **1997**, *78*, 1396.

(41) Cossi, M.; Barone, V. *J. Phys. Chem. A* **2000**, *104*, 10614–10622.

(42) (a) Wolinski, K.; Hinton, J. F.; Pulay, P. *J. Am. Chem. Soc.* **1990**, *112*, 8251–8260. (b) Helgaker, T.; Jaszunski, M.; Ruud, K. *Chem. Rev.* **1999**, *99*, 293–352. (c) Cheeseman, J. R.; Trucks, G. W.; Keith, T. A.; Frisch, M. J. *J. Chem. Phys.* **1998**, *104*, 5497–5509.